

Dalton Transactions

Accepted Manuscript

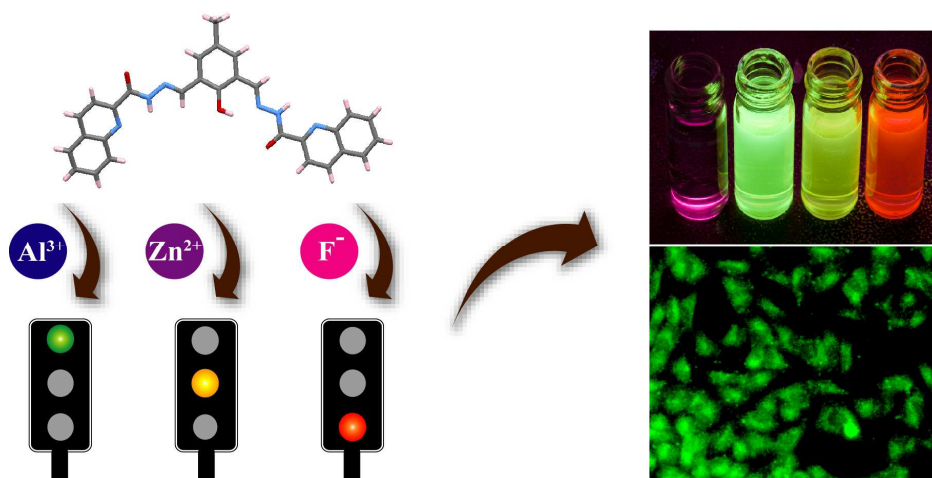


This is an *Accepted Manuscript*, which has been through the Royal Society of Chemistry peer review process and has been accepted for publication.

Accepted Manuscripts are published online shortly after acceptance, before technical editing, formatting and proof reading. Using this free service, authors can make their results available to the community, in citable form, before we publish the edited article. We will replace this *Accepted Manuscript* with the edited and formatted *Advance Article* as soon as it is available.

You can find more information about *Accepted Manuscripts* in the [Information for Authors](#).

Please note that technical editing may introduce minor changes to the text and/or graphics, which may alter content. The journal's standard [Terms & Conditions](#) and the [Ethical guidelines](#) still apply. In no event shall the Royal Society of Chemistry be held responsible for any errors or omissions in this *Accepted Manuscript* or any consequences arising from the use of any information it contains.

GRAPHICAL ABSTRACT

A dialdehyde-based ligand rendered discriminatory sensing of Al^{3+} , Zn^{2+} and F^- ions. The non-toxic receptor could also facilitate target metal sensing in live HeLa cells through imaging studies.



Journal Name

ARTICLE

A Sole Multi-Analyte receptor responds with three distinct fluorescence signals: Traffic signal like sensing of Al^{3+} , Zn^{2+} and F^-

Barun Kumar Datta,^a Durairaj Thiyagarajan,^b Aiyagari Ramesh*,^b and Gopal Das*^aReceived 00th January 20xx,
Accepted 00th January 20xx

DOI: 10.1039/x0xx00000x

www.rsc.org/

A dialdehyde-based multi-analyte sensor renders distinctive emission spectra for Al^{3+} , Zn^{2+} and F^- ions. The ligand exhibited different types of interactions with these three different ions resulting into the enhancement of fluorescence intensity at three different wavelengths. All the sensing processes were studied in details by absorption spectroscopy, emission spectroscopy and $^1\text{H-NMR}$ titration experiment. The ligand has the working ability in a wide pH range including the physiological pH. The ligand is non-toxic and amicable for sensing intracellular Al^{3+} and Zn^{2+} in live HeLa cells.

Introduction

Development of molecular sensors for selective cation or anion sensing is critical for a host of pertinent environmental, biological and diagnostic applications.¹ Amongst the cations, zinc plays a critical role in a plethora of biological processes and has significant healthcare implications.^{2,3,4} Though, there are reports of zinc sensors,⁵ still there is a need for developing new sensors that render selective detection in presence of analogous analytes such as Cd^{2+} and in biological medium. Chemists have also been actively engaged in developing Al^{3+} sensors, given the profound role of Al^{3+} in neurotoxicity and neurodegenerative diseases⁶ and its substantial impact on the environment.⁷ In the context of anions, development of fluoride-specific sensors has gained prominence, owing to its significant role in various human ailments.⁸ Although, research efforts in recent years has yielded some progress in developing fluoride sensors⁹ sensing the anion in a competitive and aqueous system still remains a formidable challenge for analytical chemists.¹⁰ With regard to the detection of environmental and biologically relevant ions, fluorescence-based tools are conceived to be efficient as they significantly enhance the capabilities for rapid and specific sensing of target analytes.^{11,c} However, the analytical merit of fluorescent sensors developed against selective ions is limited in case of multi-analyte mixtures. To address this challenge, design and application of a single probe that renders multi-analyte sensing in various formats has been reported in recent times.¹² To

develop an efficient multi-analyte sensor, it is critical to enhance the sensing repertoire of a single probe. This necessitates judicious design of the sensing ligand in order to achieve a discriminating response for various analytes.

The design principle of the reported ligand encompasses (i) incorporation of a strong fluorophore, (ii) suitable chelating ligand for binding metal ions and (iii) amide functionality for anion binding (Scheme 1). Dialdehyde derivatives are well known for their strong metal binding properties through two Schiff's base –N atoms with the hydroxyl group present at the centre of the binding cleft.^{5b,11e,11f} The hydroxyl group readily deprotonates on binding with metal ions, which switch-on the ICT process and the CHEF process. Now, in order to ensure efficient anion binding, the presence of H-bonding donor is critical. Hence, in the present study, quinoline hydrazide residue has been chosen for binding both cation and anion. Quinoline has high affinity for Al^{3+} , whereas the –NH and the –OH will offer binding site to the anions. Based on this rationale, herein, we report a single dialdehyde-based fluorescent probe, which can differentially sense Al^{3+} , Zn^{2+} and F^- ions and its distinct spectral properties upon target interaction and its application in live cell imaging studies are also reported.

Experimental Section

General Information and Materials

All the materials used for synthesis were purchased from commercial suppliers and used without further purification. 2, 6-Diformyl-4-methylphenol (DFMP) was prepared by modification of the literature method.¹³ Absorption spectra were recorded on a Perkin-Elmer Lambda-750 UV–vis spectrophotometer using 10 mm path length quartz cuvettes in the range of 250–700 nm wavelength. Fluorescence measurements were conducted on a Fluoromax-4 spectrofluorometer using 10 mm path length quartz cuvettes with a slit width of 5 nm at 298 K. All the mass spectra were

^a Department of Chemistry, Indian Institute of Technology Guwahati, Guwahati 781039, India. Fax: +91 361 2582349; Tel: +91 361 2582313 E-mail: gdas@iitg.ernet.in.

^b Department of Biosciences and Bioengineering, Indian Institute of Technology Guwahati, Guwahati 781039, India. Fax: +91 361 2582249; Tel: +91 361 2582205 E-mail: aramesh@iitg.ernet.in.

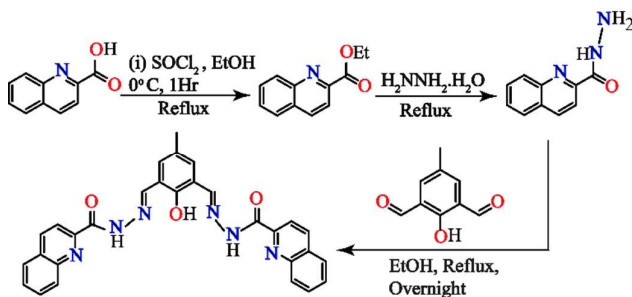
† Supporting Information

Experimental methods, compound characterization and supporting results. This material is available free of charge via the Internet at. See DOI: 10.1039/x0xx00000x

obtained using Agilent Technologies 6520 Accurate mass spectrometer. NMR spectra were recorded either on a Varian FT-400 MHz instrument or on a Bruker 600MHz instrument. The chemical shifts were recorded in parts per million (ppm) on the scale. The following abbreviations are used to describe spin multiplicities in ^1H NMR spectra: s = singlet; d = doublet; t = triplet; m = multiplet.

Synthesis of the Receptor

The synthetic route of **L** is illustrated in scheme 1. Quinaldic acid was dissolved in ethanol and in ice cold condition thionyl chloride was added drop wise over a period of 30 min with constant stirring. After 1 hour stirring, the hazy mixture was refluxed overnight. After evaporation of the solvent, water was added and the pH was adjusted to 8.0 by the addition of sodium bicarbonate. Subsequently the mixture was extracted with ethyl acetate (3x50 ml). The organic layer was dried over sodium sulphate and evaporation of the solvent gave the ethyl ester of quinaldic acid as a colourless liquid. This ester was used without further purification. This ester was then treated with excess hydrazine monohydrate in ethanol. The mixture was heated to reflux for overnight. After evaporation of the solvent and the excess hydrazine under reduced pressure, a white solid was obtained, which was dried in vacuum and was used in the next step without further purification.



Scheme 1. Synthetic route for **L**.

2,6-Diformyl-4-methylphenol (1mmol) was dissolved in ethanol. Quinaldic hydrazide (2mmol) was added to the above solution and the mixture was refluxed for 4 hours to give a yellow product. ^1H NMR [400 MHz, CDCl_3 , δ (ppm)]: 11.60 (1H, s), 11.23 (2H, s), 8.67 (2H, s), 8.37(2H, d), 8.32(2H, d), 8.17 (2H, d), 7.89 (2H, d), 7.82 (2H, q), 7.65 (3H, t), 1.69(3H,s). ^{13}C NMR [100 MHz, CDCl_3 , δ (ppm)]: 160.2, 155.8, 148.9, 146.6, 147.8, 138.0, 130.6, 129.9, 129.8, 129.1, 128.5, 128.0, 119.3, 20.4. ESI-MS (positive mode, m/z) Calculated [$\text{L} + \text{H}$] $^+$ = 503.1832, Found 503.1867.

UV-visible and Fluorescence Spectroscopic Studies

Stock solutions of various ions (1×10^{-3} mol L^{-1}) were prepared in deionized water. Perchlorate, chloride or nitrate salts of metal ions were used to prepare metal stock solutions. In case of anions tetra-butyl or tetra-ethyl ammonium salts were dissolved in deionized water to prepare the stock solutions. A stock solution of **L** (1×10^{-3} mol L^{-1}) was prepared in DMSO. The

solution of **L** was then diluted to 1×10^{-5} mol L^{-1} as required in different cases. All the spectroscopic experiments of the cations were performed in aqueous HEPES buffer medium (1 mM, pH 7.4) containing 0.33% of DMSO. In titration experiments, a solution of **L** (1×10^{-5} mol L^{-1}) was filled in a quartz optical cell of 1.0 cm optical path length, and the ion stock solutions were added gradually to achieve a concentration of 1×10^{-5} mol L^{-1} . Spectroscopic studies of **L** in presence of different anions were performed in acetonitrile medium containing 0.33% DMSO. In selectivity experiments, the test samples were prepared by interacting appropriate amounts of the cations stock into 2 mL of **L** solution (2×10^{-5} mol L^{-1}). For all the samples, the spectra were recorded following 1 min of the addition of the ions. For fluorescence measurements, excitation wavelength was set at 450 nm and emission was recorded from 460 nm to 720 nm.

Evaluation of the Apparent Binding Constants

Stock solutions of Al^{3+} and Zn^{2+} , having a concentration of 0.5×10^{-3} mol L^{-1} , in aqueous HEPES buffer (pH 7.4) solution were used. Receptor **L** with an effective concentration of 10.0×10^{-5} mol L^{-1} in the aforementioned HEPES buffer medium was used for the emission titration studies. The effective Zn^{2+} concentration was varied between 0 and 30×10^{-5} M for this titration. The solution pH was adjusted to 7.4 using an aqueous HEPES buffer solution having an effective concentration of 1.0 mM. The basic equation (1) for determination of the ligand-metal complexation is:

$$D + nM = C \quad (1)$$

where D is the ligand molecule; M is the metal ion, and C is the complex. The binding constant K of the metal complex was determined by Eq. (2), assuming the concentration of free metal is about equal to its total concentration ($[\text{M}] \approx [\text{M}]_t$),

$$I - I_0 / I - I_m = [\text{C}] / [\text{D}] = K [\text{M}]^n \quad (2)$$

where I_0 , I, and I_m are the corrected fluorescence emission intensity (at $\lambda = 500$ nm for Al^{3+} and $\lambda = 550$ nm for Zn^{2+}) of the complex at initial, interval t, and the final state at which the complex was fully formed upon addition of metal ion, respectively. The binding constant K was determined from the plot of the linear regression of $\log[(I - I_0)/(I_m - I)]$ vs. $\log[\text{M}]$ in Eq.(3), derived from Eq. (2), to obtain the intercept as $\log K$ and the slope as n:

$$\log[(I - I_0) / (I_m - I)] = \log K + n \log[\text{M}] \quad (3)$$

The apparent binding constant for the formation of the L-F complex was evaluated using the Benesi-Hildebrand (B-H) plot (equation 4).

$$1 / (I - I_0) = 1 / \{K (I_{\text{max}} - I_0) C\} + 1 / (I_{\text{max}} - I_0) \quad (4)$$

I_0 is the emission intensity of **L** at $\lambda = 575$ nm, I is the observed emission intensity at that particular wavelength in the presence of a certain concentration of ion (C), I_{max} is the maximum emission intensity value that was obtained at that λ -value during titration with varying ion concentration, K is the apparent binding constant (M^{-1}) and was determined from the slope of the linear plot, and C is the concentration of ion added during titration studies.

Detection Limit of L for different ions

The detection limit was calculated on the basis of the fluorescence titration. The fluorescence emission spectrum of L was measured 10 times, and the standard deviation of blank measurement was achieved. To gain the slopes, the ratios of the emission intensities at respective λ 's were plotted against the concentration of different ions. The detection limits were calculated using the following equation

$$\text{Detection limit} = 3\sigma/k \quad (5)$$

where σ is the standard deviation of blank measurement, and k is the slope between the ratio of emission intensity versus concentration of ion.

X-ray crystallography

Block shaped crystal of suitable size was selected from the mother liquor and immersed in silicone oil, and it was mounted on the tip of a glass fiber and cemented using epoxy resin. The intensity data were collected using a Bruker SMART APEX-II CCD diffractometer, equipped with a fine focus 1.75 kW sealed tube Mo-K α radiation ($\lambda = 0.71073 \text{ \AA}$) at 298(3) K, with increasing ω (width of 0.3° per frame) at a scan speed of 5 s per frame. The SMART software was used for data acquisition. Data integration and reduction were undertaken with SAINT and XPREP¹⁴ software. Multi-scan empirical absorption corrections were applied to the data using the program SADABS.¹⁵ Structures were solved by direct methods using SHELXS-97¹⁶ and refined with full-matrix least-squares on F2 using SHELXL-97. All non-hydrogen atoms were refined anisotropically and hydrogen atoms attached to all carbon atoms were geometrically fixed and the positional and temperature factors were refined isotropically. Structural illustrations have been drawn with MERCURY-1.3 for Windows.¹⁷

Cytotoxicity assay

The cytotoxic effect of L, L–Al complex and L–Zn complex on HeLa cells (human cervical carcinoma cells) was ascertained by MTT assay. MTT (3-(4,5-Dimethylthiazol-2-yl)-2,5-Diphenyltetrazolium Bromide) solution was procured from Sigma-Aldrich, USA. HeLa cells were initially grown in 25 cm² tissue culture flask in Dulbecco's modified Eagle medium (DMEM) supplemented with 10% (v/v) fetal bovine serum (FBS), penicillin (100g/mL) and streptomycin (100 μ g/mL) at 37°C in a CO₂ incubator. Subsequently, the cells were seeded onto 96-well tissue culture plates (approximately 10⁴ cells per well) and incubated with various concentrations of compound L, L–Al complex and L–Zn complex (10 μ M, 20 μ M, 30 μ M, 40 μ M, 50 μ M and 100 μ M) made in DMEM for a period of 24h. HeLa cells treated with DMSO or the metal salts were also included in parallel sets as control. Following 24 h incubation, the growth media was carefully aspirated and fresh DMEM containing MTT solution was added to the cells and incubated for 4 h at 37°C. Subsequently, the MTT solution was carefully removed and the insoluble colored formazan product was solubilized in DMSO and its absorbance was measured in a microtitre plate reader (Infinite M200, TECAN, Switzerland) at

550 nm. MTT assay for every sample was performed in six sets. Data analysis and calculation of standard deviation was performed with Microsoft Excel 2010 (Microsoft Corporation, USA).

Cell imaging studies

Initially HeLa cells were propagated in a 25 cm² tissue culture flask containing DMEM medium supplemented with 10% FBS, penicillin (100 μ g/mL) and streptomycin (100 μ g/mL) in a CO₂ incubator. Prior to imaging studies, the cells were seeded into a 6 well plate and grown in DMEM medium at 37°C till 80% confluency in a CO₂ incubator. Subsequently, the cells were washed thrice with sterile phosphate buffered saline (PBS) and incubated with 25 μ M L in DMEM at 37°C for 1 h in a CO₂ incubator. The cells were again washed thrice with sterile PBS to remove excess ligand and bright field and dark field images were recorded in separate sets using an epifluorescence microscope (Nikon eclipse Ti) having a filter that allowed blue light excitation and UV excitation. The cells were subsequently incubated in sterile PBS in separate sets with either 50 μ M of aluminium nitrate or 50 μ M of zinc nitrate salt for 1 h. Following incubation, the cells were washed thoroughly with sterile PBS. Bright field and dark field images of the cells were again recorded in an epifluorescence microscope using blue light excitation (green emission) for Al(III) and UV excitation (yellow emission) for Zn(II).

Results and discussion

Crystal structure of L

Block shaped single crystals of L were grown from slow evaporation of its propanol solution. It crystallizes in monoclinic system with P2₁/c space group (Z = 8). The ligand L crystallizes in monoclinic system of space group P2₁/c. Crystal structure shows two arms are not planer and stay little above the plane of central benzene ring. Close inspection in interaction pattern indicates a intramolecular H-bonding between phenolic OH and imine N-atom (O6...N8 = 2.624 \AA) is present in each asymmetric unit which possibly holds the arm tightly. We have observed a dimeric interaction between two ligand *via* carbonyl C=O and aromatic C–H H-bond (Fig. 1 and Fig. S20). Noticeably the only crystalline water molecule connects two ligand perpendicularly by donating hydrogen to quinoline N-atom atom and carbonyl C=O.



Figure 1 (a) Crystal structure of L. (b) Various non-covalent interactions in the crystal.

UV-Vis spectroscopic studies of L in the presence of metal ions

Interaction of L with various metal ions (Na^+ , K^+ , Mg^{2+} , Ca^{2+} , Co^{2+} , Ni^{2+} , Cu^{2+} , Cd^{2+} , Ag^+ , Pb^{2+} , Hg^{2+} , Al^{3+} , Cr^{3+} , Fe^{3+} , Zn^{2+}) was pursued in a HEPES buffer medium (5 mM, pH 7.4) containing 0.33% of DMSO. The receptor exhibited three characteristic peaks at 289 nm ($\epsilon = 4.67 \times 10^4 \text{ M}^{-1} \text{ cm}^{-1}$), 315 nm ($\epsilon = 3.96 \times 10^4 \text{ M}^{-1} \text{ cm}^{-1}$) and at 368 nm ($\epsilon = 2.65 \times 10^4 \text{ M}^{-1} \text{ cm}^{-1}$), originating from π - π^* transitions and the long conjugation present in the free ligand system. Amongst various metal ions (10 equivalent of each), interaction with Al^{3+} , Zn^{2+} , and Cu^{2+} only resulted in a change in the absorption spectra of L, with the maximum change observed with Zn^{2+} (ESI,† Fig. S1). Titration experiment with gradual addition of Al^{3+} ions resulted in diminishing of the peaks at 289 nm, 315 nm and 368 nm along with the emergence of a new peak at 430 nm ($\epsilon = 1.97 \times 10^3 \text{ M}^{-1} \text{ cm}^{-1}$ for Al^{3+} and $\epsilon = 1.51 \times 10^4 \text{ M}^{-1} \text{ cm}^{-1}$ for Zn^{2+}) (Fig. 2(A)), which can be attributed to the strong ligand-to-metal charge-transfer (LMCT). Presence of isosbestic points at 337 nm and 395 nm established the transformation of free receptor in its aluminium complex (Fig. 2(A)). Titration experiment with Zn^{2+} yielded analogous results as in the case of Al^{3+} , albeit a change of higher magnitude (Fig. 2(B)). Interestingly, a visual colour change from colourless to light yellow and deep yellow were observed with Al^{3+} and Zn^{2+} , respectively (Fig. 2(A), inset).

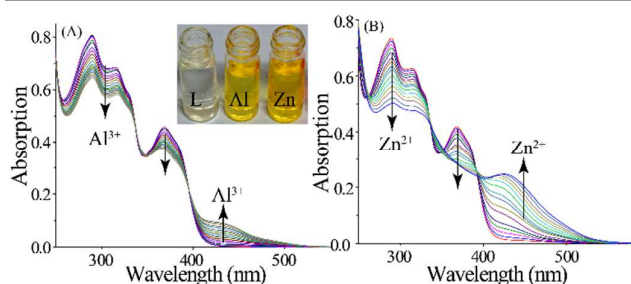


Figure 2. Changes in absorption spectra of L (25 μM) with (A) the incremental addition of Al^{3+} . Inset: colour change upon the addition of Al^{3+} and Zn^{2+} to L, (B) the incremental addition of Zn^{2+} .

Fluorescence spectroscopic studies of L in the presence of metal ions

When excited at 450 nm, L displayed a weak emission peak at 520 nm. In presence of a set of metal ions (Na^+ , K^+ , Mg^{2+} , Ca^{2+} , Co^{2+} , Ni^{2+} , Cu^{2+} , Cd^{2+} , Ag^+ , Pb^{2+} , Hg^{2+} , Al^{3+} , Cr^{3+} , Fe^{3+} , Zn^{2+}) in a buffered solution, a remarkable enhancement in the emission spectra of L was observed only with Al^{3+} and Zn^{2+} at two distinct wavelengths corresponding to 500 nm and 550 nm, respectively (ESI,† Fig. S2). These results validated the selectivity of L towards Al^{3+} and Zn^{2+} . Consequently, green fluorescence was observed in case of Al^{3+} whereas greenish yellow fluorescence was observed upon interaction with Zn^{2+} (ESI, † Fig. S2, inset). Titration experiments were also performed with gradual addition of Al^{3+} and Zn^{2+} to the solution of L. In both the cases, a systematic increment in the emission intensity of L was observed (Fig. 3). It may be mentioned that in both cases, enhancement in emission

intensity of L became minimal after the addition of two equivalents of the target metal ions (Fig. 3, inset). Further from the UV/Vis absorption spectra isosbestic points were observed at 337 nm, 395 nm and 395 nm respectively. Using the higher wavelength isosbestic point (395 nm) as excitation wavelength for emission experiments, analogous results were obtained for the target metals. Job's plot obtained from the titration experiments yielded 1:2 stoichiometry for both Al^{3+} and Zn^{2+} (ESI,† Fig. S7- S8). The association constant of L for Al^{3+} and Zn^{2+} derived from Bensei-Hildebrand plot^{13, 11f} (ESI,† Fig. S9-S10) was observed to be $1.07 \times 10^5 \text{ M}^{-2}$ and $1.75 \times 10^5 \text{ M}^{-2}$, respectively. The detection limit of L for Al^{3+} and Zn^{2+} was 32 ppb and 35 ppb, respectively. The quantum yield of the free receptor was 0.002 whereas quantum yields for L-Al and L-Zn complexes were found to be 0.42 and 0.54 respectively. The selectivity of L towards Al^{3+} and Zn^{2+} was also established through experiments in the presence of competing metal ions (ESI,† Fig. S5-S6).

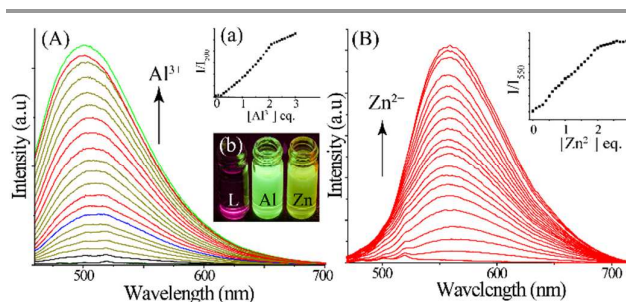


Figure 3. Changes in emission spectra of L (25 μM) (A) with the incremental addition of Al^{3+} . Inset: (a) Intensity at 500 nm vs $[\text{Al}^{3+}]$ plot, (b) Visual colour change upon the addition of Al^{3+} and Zn^{2+} to L under UV lamp ($\lambda_{\text{ex}} = 365 \text{ nm}$). (B) with incremental addition of Zn^{2+} , Inset: Intensity at 550 nm vs $[\text{Zn}^{2+}]$ plot.

UV-Vis spectroscopic studies of L in the presence of anions

To ascertain the sensing potential of L towards multi-target analyte, spectroscopic studies in presence of different anions were performed in an acetonitrile medium with 0.33% DMSO as a co-solvent. Among a set of different anions (F^- , Cl^- , Br^- , OH^- , I^- , NO_3^- , HSO_3^- , SO_4^{2-} , ClO_4^- , ClO_3^- , CN^- , S_2^- , H_2PO_4^- , PO_4^{3-}), a prominent change in the absorption spectra of L was manifested only upon addition of F^- (ESI,† Fig. S3). Titration of L with incremental amount of F^- resulted in a systematic decrease in the absorption peak at 368 nm and emergence of a new peak at 506 nm (Fig. 4A). Two distinct isosbestic points at 340 nm and 395 nm in the titration spectra indicated the formation of a new species. Interestingly, the colour of the solution changed from colourless to orange during the titration process (Fig. 4A, inset).

Fluorescence spectroscopic studies of L in the presence of anions

When a set of various anions was used as target analyte, only F^- imparted a change in the emission spectra of L while other anions failed to induce any variation (ESI,† Fig. S4). Titration of

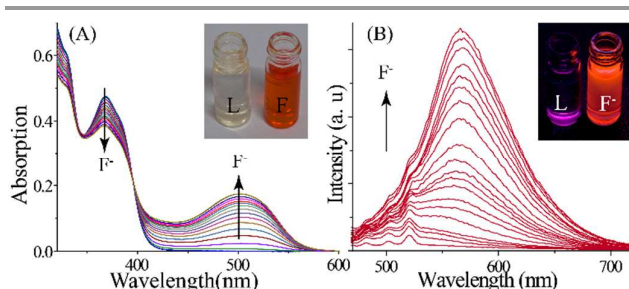


Figure 4. Changes in (A) absorption spectra of L (25 μM) with the incremental addition of F^- . Inset: Visual colour change upon the addition of F^- to L, (B) emission spectra of L (25 μM) with the incremental addition of F^- . Inset: Visual colour change upon the addition of F^- to L under UV lamp ($\lambda_{\text{ex}} = 365 \text{ nm}$).

L with fluoride triggered a distinct enhancement in the emission intensity at 575 nm and the fluorescence of the solution also changed to bright orange (Fig. 4B, inset). Jobs plot derived from the titration process revealed a 1:1 stoichiometry between L and F^- . The receptor L could detect F^- as low as 40 ppb. The quantum yield of the free receptor was 0.002 whereas quantum yield for L- F^- ensemble was calculated to be 0.40. The spectral and colour change were due to the formation of receptor-fluoride H-bonded complex. This phenomenon was validated by addition of a small volume of water/methanol, which yielded a colourless solution.

pH dependent study

At lower pH (2-5), L was unable to sense any of the metal ions due to the protonation of the receptor. In the pH range of 5.5-9.5, the sensing behaviour of L towards both the metal ions was robust. At pH greater than 10, L could only recognize Zn^{2+} through a turn-on response. Interestingly, the receptor displayed stable fluorescence at physiological pH (ESI,† Fig. S11), which suggested that the receptor is likely to be amicable for sensing in the physiological microenvironment and cellular milieu.

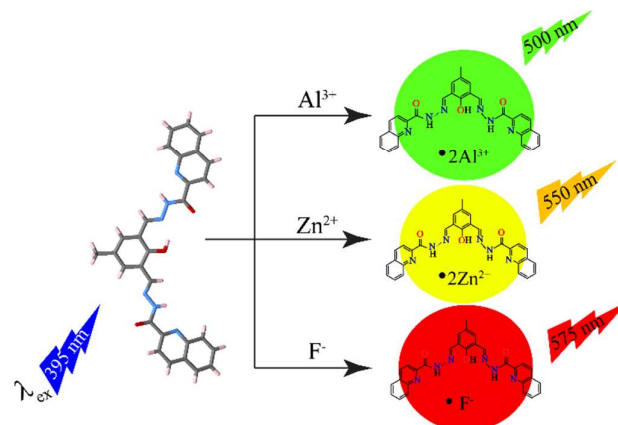
$^1\text{H-NMR}$ titration experiment of L in presence of Al^{3+} , Zn^{2+} and F^-

To probe the interaction between L with Al^{3+} and Zn^{2+} , $^1\text{H-NMR}$ titration experiment was performed for both the metal ions. Titration of L with Al^{3+} resulted in upfield shift for $-\text{NH}$ (0.020 ppm), $-\text{OH}$ (0.049 ppm) and the Schiff base protons (0.056 ppm) (ESI,† Fig. S17). In case of titration with Zn^{2+} similar trends of lesser magnitude were observed (ESI,† Fig. S18). With the gradual addition of Zn^{2+} , the reduction in intensity of $-\text{OH}$ group peak was accompanied by an upfield shift, which indicated deprotonation of L. The above results strongly indicated that the phenolic $-\text{OH}$ group and the Schiff base N-atoms bind with both the metal ions along with the deprotonation of the phenolic $-\text{OH}$ group. Involvement of the quinoline ring in binding with Al^{3+} was clear from the shifts of the quinoline ring protons whereas in the case of Zn^{2+} , quinoline ring did not participate in binding which was also evident from the $^1\text{H-NMR}$ experiment. The changes in the $^1\text{H-NMR}$ spectra of L were observed up to the addition of two equivalents of Zn^{2+} ions, which supported the results obtained

from the absorption and emission spectroscopy. $^1\text{H-NMR}$ titration of L with tetra-butyl salt of fluoride yielded prominent changes in comparison with the metal ions (ESI,† Fig. S19). Deprotonation of both the phenolic $-\text{OH}$ group and the $-\text{NH}$ group was observed on the addition of excess of F^- ion. Initially the phenolic $-\text{OH}$ group, was deprotonated and a downfield shift along with reduction in the intensity of the $-\text{NH}$ proton was observed ($\Delta\delta = 0.055 \text{ ppm}$). The imine proton also confronted downfield shift of $\Delta\delta = 0.116 \text{ ppm}$, whereas the quinoline ring protons were shifted upfield but the shifts ($\Delta\delta$) were miniscule compared to the other changes. So, due to deprotonation of both the phenolic $-\text{OH}$ and the $-\text{NH}$ groups, sharp changes were observed in the case of fluoride in both absorption and emission spectroscopy.

Plausible Mechanism of sensing

The low fluorescence of the free receptor may be attributed to the absence of intramolecular charge transfer (ICT) and the free rotation around the imine bond. Upon interaction with the target analytes, the free rotation around the imine bonds got restricted, which resulted in the formation of a rigid platform. Hence, chelation enhanced fluorescence (CHEF) process occurred in the presence of the analytes. Further, in all cases, deprotonation triggers the ICT process, which leads to the turning-on of the fluorescence of the receptor. Moreover, a difference in charge density of the cations likely to affect the ICT mechanism as the ligand is directly involved in binding with the cations. This may account for the change in emission maximum of the probe upon interaction with Al(III) and Zn(II) .



Scheme 2: Schematic representation of sensing of Al^{3+} , Zn^{2+} and F^- by L.

Biological studies of L in the presence of metal ions

On the basis of the excellent response of L towards Al^{3+} and Zn^{2+} in solution mimicking the physiological condition, we anticipated that L could be explored for the sensing of these

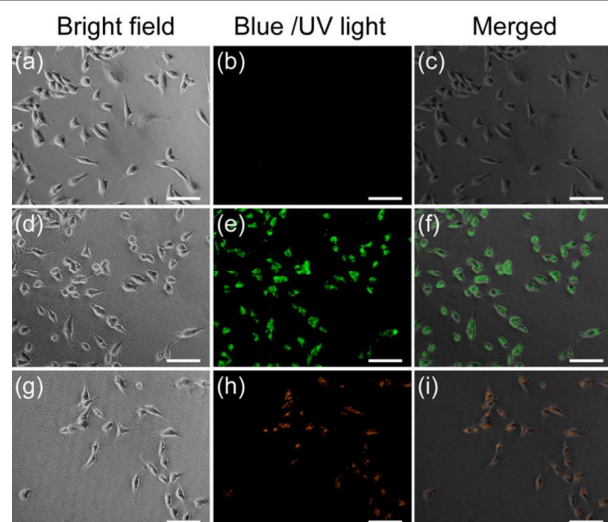


Figure 5. Fluorescence microscopic images of HeLa cells treated with (A-C) 5.0 μM of L, (D-F) pre-treated with 5.0 μM of L followed by addition of 50 μM Al^{3+} solution, (G-I) pre-treated with 5.0 μM of L followed by addition of 50 μM Zn^{2+} solution. Scale bar for the images is 100 μM .

target metals in live cells. To accomplish this goal, it was significant to probe the cytotoxic effect of L and its metal complexes on live cells. A conventional MTT assay, which is based on the mitochondrial dehydrogenase activity of viable cells illustrated that L as well as the metal complexes failed to affect the viability of the HeLa cells even at a concentration as high as 50 μM (ESI,† Fig. S12). Subsequently, sensing of Al^{3+} and Zn^{2+} was pursued in HeLa cells by cell imaging studies, wherein the cells were initially incubated with 10 μM of L followed by addition of 20 μM each of either Al^{3+} or Zn^{2+} in separate sets. HeLa cells incubated with only L failed to exhibit any fluorescence. Upon incubation with $\text{Al}(\text{III})$ and using blue excitation, bright green fluorescence manifested in the cells (Fig. 5). Interestingly, in case of $\text{Zn}(\text{II})$, when HeLa cells were subjected to UV excitation, a yellowish-orange fluorescence was conspicuous in the cells (Fig. 5). These results were significant and highlight the analytical merit of L as the probe could differentiate $\text{Al}(\text{III})$ and $\text{Zn}(\text{II})$ in the complex biological milieu, akin to earlier results obtained in solution-based experiments (Fig. 3). It was also noted that the fluorescence emission obtained for both the target metals was well spread in the cell, which suggested that the ligand could traverse across the cell membrane and diffuse throughout the cell. It was also evident that the HeLa cells retained their morphological trait during the cell imaging studies (Fig. 5), which reiterated the non-toxic nature of the developed receptor.

Conclusion

In brief, we have designed and synthesized a new di-aldehyde-based sensor, which facilitates distinctive sensing of Al^{3+} , Zn^{2+} and F^- . The present work is a judicious illustration of

developing a single fluorescence-based probe for multi-analytes, which may render useful applications in environmental and diagnostic regime.

Acknowledgements

We thank the SERB (SR/S1/OC-62/2011), CSIR (01/2727/13/EMR-II) and DBT (BT/01/NE/PS/08) for research grants and Central Instruments Facility, IIT Guwahati, for their help in NMR analysis. BKD and DT thank IIT Guwahati, for research fellowship. Special thanks to Md. Najbul Hoque and Romen Chutia for their coordination with the crystallography part.

Notes and References

Crystallographic data of L:- Empirical formula: $\text{C}_{29}\text{H}_{22}\text{N}_6\text{O}_4$, MW: 518.53, T = 298 (2) K, monoclinic space group: P21/c, a=21.318(3) $^\circ\text{A}$, b=11.3583(13) $^\circ\text{A}$, c=21.294(3) $^\circ\text{A}$, β =92.519(7) $^\circ$, V = 5151.1(11) A^3 , Z = 5, Dx (g cm $^{-3}$)=1.337, m=0.092 mm $^{-1}$, F(000)=2110, reflections collected/unique = 12124/7351, R1 = 0.0630, wR2 = 0.1165 [$I > 2\sigma(I)$], R1 = 0.2639, wR2 = 0.1661 (all data), GOF(F2) = 0.993. CCDC No. 1060275.

- (a) D. Astruc, E. Boisselier and C. Ornelas, *Chem. Rev.*, 2010, **110**, 1857- 1959; (b) J. Wu, W. Liu, J. Ge, H. Zhang and P. Wang, *Chem. Soc. Rev.*, 2011, **40**, 3483- 3495. (c) A. P. de Silva, H. Q. N. Gunaratne, T. Gunnlaugsson, A. J. M. Huxley, C. P. McCoy, J. T. Rademacher and T. E. Rice, *Chem. Rev.*, 1997, **97**, 1515- 1566.
- (a) K. M. Hambidge and N. F. Krebs, *J. Nutr.*, 2007, **137**, 1101-1105; (b) J. M. Berg and Y. Shi, *Science*, 1996, **271**, 1081-1085; (c) A. C. Burdette and S. J. Lippard, *Proc. Natl. Acad. Sci. U. S. A.*, 2003, **100**, 3605–3610.
- (a) S. Y. Assaf and S. H. Chung, *Nature*, 1984, **308**, 734–736; (b) C. J. Frederickson and A. I. Bush, *BioMetals*, 2001, **14**, 353-366; (c) P. Molnar, J. V. Nadler, *Brain Res.*, 2001, **910**, 205-207; (d) A. M. Hosie, E. L. Dunne, R. J. Harvey and T. G. Smart, *Nat. Neurosci.*, 2003, **6**, 362–369.
- (a) J. Y. Koh, S. W. Suh, B. J. Gwag, Y. Y. He, C. Y. Hsu and D. W. Choi, *Science*, 1996, **272**, 1013-1016; (b) C. Sindreu, R. D. Palminter and D. R. Storm, *Proc. Natl. Acad. Sci. U. S. A.*, 2011, **108**, 3366–3370; (c) A. I. Bush, *Alzheimer Dis. Assoc. Disord.*, 2003, **17**, 147–150; (d) C. J. Frederickson, J. Y. Koh and A. I. Bush, *Nat. Rev. Neurosci.*, 2005, **6**, 449–462.
- (a) Z. Xu, J. Yoon and D. R. Spring, *Chem. Soc. Rev.*, 2010, **39**, 1996-2006; (b) B. K. Datta, S. Mukherjee, C. Kar, A. Ramesh and G. Das, *Anal. Chem.*, 2013, **85**, 8369–8375; (c) Y. Mikata, A. Yamashita, K. Kawata, H. Konno, S. Itami, K. Yasuda and S. Tamotsu, *Dalton Trans.*, 2012, **41**, 4976–4984; (d) J. E. Kwon, S. Lee, Y. You, K.-H. Baek, K. Ohkubo, J. Cho, S. Fukuzumi, I. Shin, S. Y. Park and W. Nam, *Inorg. Chem.*, 2012, **51**, 8760–8774.
- (a) A. Salifoglou, *Coord. Chem. Rev.*, 2002, **228**, 297–317; (b) M. E. Percy, T. P. A. Kruck, A. I. Pogue and W. J. Lukiw, *J. Inorg. Biochem.*, 2011, **105**, 1505–1512; (c) G. D. Fasman, *Coord. Chem. Rev.*, 1996, **149**, 125–165; (d) D. Krewski, R. A. Yokel, E. Nieboer, D. Borchelt, J. Cohen, J. Harry, S. Kacew, J. Lindsay, A. M. Mahfouz and V. Rondeau, *J. Toxicol. Environ. Health, Part B.*, 2007, **10(S1)**, 1-269.
- (a) E. Altschuler, *Med. Hypotheses*, 1999, **53**, 22-23; (b) S. Polizzi, E. Pira, M. Ferrara, M. Bugiani, A. Papaleo, R. Albera and S. Palmi, *NeuroToxicology*, 2002, **23**, 761–774; (c) H. E. Witters, S. VanPuymbroeck, A. H. X. Stouthart and S. E. W.

- Bonga, *Environ. Toxicol. Chem.*, 1996, **15**, 986–996; (d) L. V. Kochian, O. A. Hoekenga and M. A. Piñeros, *Annu. Rev. Plant Biol.*, 2004, **55**, 459–493; (e) A. B. S. Poléo, K. Østbye, S. A. Øxnevad, R. A. Andersen, E. Heibo and L. A. Vøllestad, *Environ. Pollut.*, 1997, **96**, 129–39.
- 8 (a) E. Gazzano, L. Bergandi, C. Riganti, E. Aldieri, S. Doublier, C. Costamagna, A. Bosia and D. Ghigo, *Curr. Med. Chem.*, 2010, **17**, 2431–2441; (b) B. Spittle, Neurotoxic effects of fluoride, *Fluoride*, 2011, **44**, 117–124; (c) P. Grandjean and P. J. Landrigan, *Lancet.*, 2006, **368**, 2167–2178.
- 9 (a) M. Cametti and K. Rissanen, *Chem. Commun.*, 2009, 2809–2829; (b) S.-D. Jeong, A. Nowak-Krol, Y. Kim, S.-J. Kim, D. T. Gryko and C.-H. Lee, *Chem. Commun.*, 2010, **46**, 8737–8739; (c) T. Mizuno, W.-H. Wei, L. R. Eller and J. L. Sessler, *J. Am. Chem. Soc.*, 2002, **124**, 1134–1135; (d) J. Wang, L. Yang, C. Hou and H. Cao, *Org. Biomol. Chem.*, 2012, **10**, 6271–6274; (e) I.-S. Ke, M. Myahkostupov, F. N. Castellano and F. P. Gabbai, *J. Am. Chem. Soc.*, 2012, **134**, 15309–15311.
- 10 (a) J. L. Sessler, P. A. Gale and W. S. Cho, *Anion Receptor Chemistry*; Royal Society of Chemistry: Cambridge, UK, 2006. (b) W. J. Marshall and S. K. Bangert, *Clinical Chemistry*, Elsevier: Edinburgh, 5th ed.; 2004.
- 11 (a) G. Aragay, J. Pons and A. Merkoç, *Chem. Rev.*, 2011, **111**, 3433–3458; (b) K. M. Dean, Y. Qin and A. E. Palmer, *Biochim. Biophys. Acta*, 2012, **1823**, 1406–1415; (c) S. Samanta, S. Goswami, A. Ramesh and G. Das, *Sens. Actuators, B*, 2014, **194**, 120–126; (d) C. Kar, M. D. Adhikari, A. Ramesh and G. Das, *Inorg. Chem.*, 2013, **52**, 743–752; (e) B. K. Datta, D. Thiyagarajan, C. Kar, A. Ramesh and G. Das, *Org. Biomol. Chem.*, 2014, **12**, 4975–4982; (f) C. Kar, M. D. Adhikari, B. K. Datta, A. Ramesh and G. Das, *Sens. Actuators, B.*, 2013, **188**, 1132–1140.
- 12 (a) D. C. Magri, G. J. Brown, G. D. McClean and A. P. de Silva, *J. Am. Chem. Soc.*, 2006, **128**, 4950–4951; (b) A. P. de Silva and S. Uchiyama, *Nat. Nanotechnol.*, 2007, **2**, 399–410; (c) D. Margulies, C. E. Felder, G. Melman, A. Shanzer, *J. Am. Chem. Soc.*, 2007, **129**, 347–354; (d) M. Dong, Y. Peng, Y.-M. Dong, N. Tang and Y.-W. Wang, *Org. Lett.*, 2012, **14**, 130–133; (e) L. E. Santos-Figueroa, M. E. Moragues, E. Climent, A. Agostini, R. Martinez-Manez, F. Sanceno'n, *Chem. Soc. Rev.*, 2013, **42**, 3489–3613.
- 13 H. A. Benesi and J. H. Hildebrand, *J. Am. Chem. Soc.*, 1949, **71**, 2703–2707.
- 14 *Saint, Smart and XPREP*, Siemens Analytical X-ray Instruments Inc., Madison, Wisconsin, USA, 1995.
- 15 G. M. Sheldrick, *SADABS: software for Empirical Absorption Correction*, University of Gottingen, Institute für Anorganische Chemie der Universität, Tammanstrasse 4, D-3400 Gottingen, Germany, 1999–2003.
- 16 (a) G. M. Sheldrick, *SHELXS-97*, University of Gottingen, Germany, 1997; (b) G. M. Sheldrick, *SHELXL-97, Program for Crystal Structure Refinement*, University of Gottingen, Germany, 1997.
- 17 *Mercury 1.3 Supplied with Cambridge Structural Database*, CCDC, Cambridge, U.K., 2003–2004.